Optoelectronic Devices Grown on Nonpolar and Semipolar Free-Standing GaN Substrates

Daniel Feezell, James Speck, Steven DenBaars, and Shuji Nakamura

Materials Department, University of California, Santa Barbara, CA 93106-9560
*Email: feezell@engineering.ucsb.edu; Tel: +1-805-893-4362

Keywords: GaN, light-emitting diode, laser diode, nonpolar, semipolar

Abstract

Recently, considerable research effort has been applied to the development of optoelectronic devices on nonpolar and semipolar free-standing GaN substrates. The major driving force behind this effort is the realization of laser diodes (LDs) and light-emitting diodes (LEDs) with improved optical efficiency, particularly in the violet, blue, and green spectral regions. The principle markets for these sources include data storage, projection displays, and general lighting. We present a summary of materials and device development for LDs and LEDs grown on several orientations of nonpolar and semipolar free-standing GaN. The novel crystal orientations explored in this work result in devices that may offer several performance benefits over conventional *c*-plane (polar) technology.

INTRODUCTION

III-Nitride optoelectronic devices have achieved remarkable progress since their commercial introduction nearly twenty years ago. Advanced epitaxial growth, sophisticated fabrication techniques, and novel device designs have resulted in high-performance light-emitting diodes (LEDs) and laser diodes (LDs) for a range of applications. GaN-based LEDs have experienced considerable success in solid-state lighting (SSL) and displays, while GaN-based LDs are utilized for optical data storage and are desirable for projection displays and optical sensing.

All commercially available GaN-based devices are grown along the polar *c*-axis of the wurtzite crystal. In these structures, spontaneous and piezoelectric polarizations induce electric fields in the structure that are perpendicular to the growth direction, resulting in tilted energy bands [1]. These electric fields spatially separate the electron and hole wave functions in the quantum wells (QWs), limiting the optical efficiency of *c*-plane devices [2]. Additionally, the Quantum-Confined Stark Effect causes the peak emission wavelength to decrease (blue-shift) with increasing drive current. These issues are particularly problematic for higher $In_xGa_{1-x}N$ alloy compositions due to the strain dependence of piezoelectric polarization. Consequently, efficient optical devices in the green spectral region, which are desirable for SSL and displays, are difficult to achieve.

One approach to mitigate these problems is the growth of structures on nonpolar/semipolar orientations [3]. Nonpolar orientations are essentially free from polarization-related electric fields, whereas semipolar orientations have greatly reduced fields. As a result, optical devices fabricated on these alternative orientations are predicted to have higher radiative efficiencies than *c*-plane devices and to exhibit minimal blue-shift with increasing current density [4]. Superior performance in the green spectral is also an attractive possibility. Select semipolar planes are predicted to have increased indium uptakes [5] and compositional homogeneity [6].

Although nonpolar/semipolar III-Nitride technology is still relatively immature, recent results highlight its considerable potential for producing high-efficiency optical devices [7-9]. Researchers have rapidly improved these novel structures and demonstrated LEDs and LDs spanning from the violet to green regions of the optical spectrum. In this work, we present a summary of recent nonpolar/semipolar LD and LED results achieved in the Solid State Lighting and Energy Center (SSLEC) at the University of California Santa Barbara (UCSB).

SUBSTRATES AND EPITAXY

The reduction of dislocation density is regarded as an important step toward improving III-Nitride device performance. We have therefore used free-standing GaN substrates for all of the LEDs and LDs presented in the following sections. These substrates are manufactured by Mitsubishi Chemical Corporation. They are grown by hydride vapor phase epitaxy (HVPE) in the *c*-direction and then sliced to expose either a nonpolar or semipolar plane. The surface is then rendered epitaxy-ready by chemical-mechanical polishing. The resulting substrates have threading dislocation densities of less than 5×10^6 cm^{-2}.

All epitaxial layers were grown by atmospheric pressure metal organic chemical vapor deposition (MOCVD) using conditions similar to those required for optimized *c*-plane structures.

NONPOLAR/SEMIPOLAR LIGHT-EMITTING DIODES

The Department of Energy (DOE) predicts that, by 2030, SSL has the potential to reduce electricity consumption for lighting in the United States (which accounts for 25% of the total consumption) by over 25% — translating to a cost savings of more than $120 billion at today's energy prices or to the equivalent reduction of 2.6 billion barrels of oil [10]. The adoption of SSL would be greatly accelerated by improvements to the internal quantum efficiencies (IQEs) of

TABLE I

PERFORMANCE CHARACTERISTICS FOR LEDS GROWN ON SEVERAL SEMIPOLAR ORIENTATIONS. ALL DATA COLLECTED UNDER PULSED CONDITIONS WITH 1% DUTY CYCLE.

Orientation / Color / Substrate	λ (nm)	I (mA)	Chip Area (um²)	J (A/cm²)	LOP (mW)	EQE (%)
(20$\underline{2}$1) / Blue / GaN	432	350	500 x 2000	35	296.6	29.5
(10$\underline{1}$1) / Blue / GaN	432	350	500 x 2000	35	458.0	45.6
(20$\underline{2}$1) / Blue / GaN	451	350	500 x 2000	35	404.2	42.0
(30$\underline{3}$1) / Blue / GaN	452	20	500 x 200	20	14.5	26.4
(11$\underline{2}$2) / Green / GaN	516	20	200 x 550	18	5.0	10.4
(20$\underline{2}$1) / Green / GaN	516	20	292 x 490	14	9.9	20.6
(20$\underline{2}$1) / Green-Yellow / GaN	552	20	292 x 490	14	5.7	12.7
(11$\underline{2}$2) / Yellow / GaN	563	20	600 x 450	7	5.9	13.4

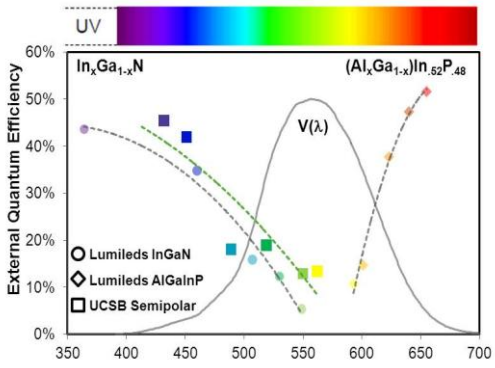

Figure 1: External quantum efficiency (EQE) vs. peak wavelength for $In_xGa_{1-x}N$ and $(Al_xGa_{1-x})In_{.52}P_{.48}$ LEDs illustrating the efficiency dip in the green region. Commercially available *c*-plane LEDs are also plotted for comparison.

LEDs, particularly at high current densities, at high temperatures, and in the green spectral region.

Researchers in the SSLEC have recently been exploring LEDs on a variety of semipolar orientations with the goal of improving several critical performance metrics, including IQE, light extraction efficiency, thermal sensitivity, and droop. Table I illustrates the basic performance characteristics for blue, green, and yellow LEDs grown on several semipolar orientations at UCSB. These results will be further detailed in the accompanying conference presentation.

Our initial results indicate that nonpolar/semipolar orientations may provide a path to address several critical issues that currently limit the performance of III-Nitride LEDs. One example is the well-documented reduction of optical efficiency as a function of increasing indium mole fraction in $In_xGa_{1-x}N$ alloys [11]. This phenomenon is often referred to as the "green gap," a phrase that is derived from the general absence of high-efficiency optical devices in the green spectral region. Figure 1 shows external quantum efficiency (EQE) vs. wavelength for $In_xGa_{1-x}N$ and $(Al_xGa_{1-x})In_{.52}P_{.48}$ LED technologies and illustrates the efficiency dip in the green region. For $In_xGa_{1-x}N$ devices, the figure compares data between industry LEDs (non-thin-film-flip-chip from Philips Lumileds) and recent results from UCSB's semipolar LEDs on (11$\underline{2}$2) and (10$\underline{1}$1) orientations. Although the results for UCSB's semipolar LEDs are only university-level demonstrations with very basic light extraction techniques, the performance is competitive across the blue to yellow region.

Another issue that we are exploring with nonpolar/semipolar III-Nitrides is the reduction of optical efficiency that is observed as a function of increasing carrier density, often referred to as "efficiency droop." The physical origin of this phenomenon is highly debated and is currently the focus of substantial research. Some proposed mechanisms are Auger recombination, carrier delocalization from compositional fluctuations, carrier leakage from the active region, and polarization-related electric fields [12-16]. A solution to efficiency droop would allow devices to maintain peak efficiencies over a wide range of operating conditions, facilitate scaling of chip sizes to smaller dimensions, and relax restrictions on epitaxial material design and quality. We are therefore tracking droop performance on all of our LEDs. Figure 2 shows the droop characteristics of blue LEDs on several semipolar orientations and Table II shows the associated droop data. Due to the reduced polarization-related electric fields on nonpolar/semipolar planes, optically efficient device with increased QW thickness can be realized. This design flexibility may offer opportunities to reduce both electrical and thermal droop by allowing for reduced carrier densities in the active region.

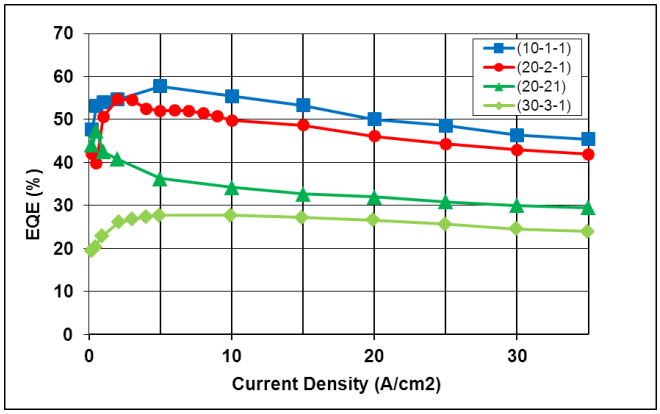

Figure 2: External quantum efficiency vs. current density for blue LEDs on several semipolar orientations.

TABLE II

DROOP CHARACTERISTICS FOR SEMIPOLAR LEDS SHOWN IN FIGURE 2.

Orientation	Wavelength (nm)	Peak EQE (%)	EQE @ 35 A/cm² (%)	Droop
(10$\underline{1}$1)	432	57.8	45.4	21.4 %
(20$\underline{2}$1)	451	54.7	41.9	23.4 %
(20$\underline{2}$1)	432	47.3	29.5	37.6 %
(30$\underline{3}$1)	456	27.7	24.0	13.4 %

NONPOLAR/SEMIPOLAR LASER DIODES

Researchers in the SSLEC are also focused on the development of violet, blue, and green LDs grown on nonpolar/semipolar GaN. These devices are primarily based on our previously-reported AlGaN-cladding-free waveguide design [17]. In the blue and green regions of the optical spectrum there is growing interest in direct-injection LDs for laser-based displays and projectors. In these applications, laser sources allow for a wide color gamut, high definition, and low power consumption. The use of these novel orientations is predicted to provide several advantages over conventional *c*-plane laser diodes including increased optical gain and lower threshold current density [4], which may facilitate higher performance LDs, particularly in the blue and green spectral regions. Recent reports from commercial industry highlight the strong performance characteristics of nonpolar/semipolar laser diodes [7,18]. Researchers in the SSLEC have recently demonstrated violet LDs with low threshold current densities and continuous wave (CW) blue laser diodes on nonpolar (m-plane) [19], and green LDs on semipolar substrates. Table III summarizes the most recent results, which will be further detailed in the accompanying conference presentation.

Until recently threshold current densities for nonpolar/semipolar LDs remained two to three times higher than those of *c*-plane LDs. Emerging evidence now suggests that nonpolar/semipolar LDs can at least equal, and quite possibly outperform, state-of-the-art *c*-plane LDs. In the SSLEC, researchers have demonstrated violet nonpolar LDs with threshold current densities as low as 1.54 kA/cm^2 [20]. This is comparable to the lowest threshold current density reported on *c*-plane LDs. Figure 3 shows threshold current density vs. wavelength for nonpolar, semipolar, and *c*-plane LDs. Despite the relative level of immaturity of nonpolar/semipolar LDs, their performance is now comparable to or better than that of c-plane LDs, particularly in the true-green region.

A semipolar orientation that has recently shown particular promise for green LDs is (20$\underline{2}$1), which is angled approximately 15^o off of the (10$\underline{1}$0) m-plane toward (000$\underline{1}$) [7]. This orientation has approximately one-fourth of the polarization-related electric field intensity as *c*-plane and has demonstrated an increased ability for indium uptake during crystal growth. Additionally, time-resolved photoluminescence (TRPL) studies have shown that green-emitting quantum wells on (20$\underline{2}$1) have superior compositional homogeneity to those on *c*-plane [6]. Researchers in the SSLEC have utilized semipolar (20$\underline{2}$1) substrates to achieve one of the few university demonstrations of a true-green III-Nitride LD [21]. These devices had a peak wavelength of 516 nm. In these structures AlGaN barriers were shown to improve emission uniformity and to increase spontaneous emission output power, likely due to strain compensation. Figure 4 shows the far field image of the semipolar green LD developed at UCSB.

TABLE III

PERFORMANCE CHARACTERISTICS FOR NONPOLAR AND SEMIPOLAR LASERS DIODES DEVELOPED AT UCSB

Orientation / Color	λ (nm)	Operating Condition	Jth (kA/cm^2)	Maximum P_{out} (mW)
(10$\underline{1}$0) Nonpolar / Violet	413	Pulsed	1.5	200
(10$\underline{1}$0) Nonpolar / Violet	411	Pulsed	4.7	1600
(30$\underline{3}$1) Semipolar / Blue	445	Pulsed	5.7	100
(10$\underline{1}$0) Nonpolar / Blue	461	CW	4.1	6
(20$\underline{2}$1) Semipolar / Green	516	Pulsed	30.0	7.5

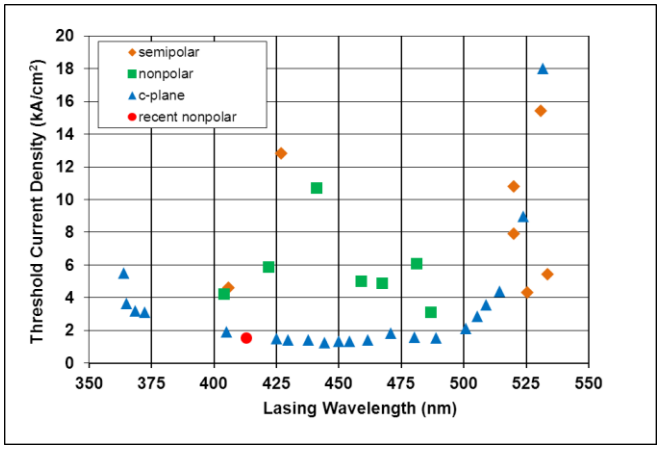

Figure 3: Threshold current density vs. lasing wavelength for nonpolar, semipolar, and c-plane laser diodes. Figure after reference [20].

CONCLUSIONS

In summary, we have presented the recent performance of nonpolar/semipolar LEDs and LDs developed in the SSLEC at UCSB. We have examined the potential of several semipolar orientations for LEDs with higher efficiency in the green region and improved droop performance. We have also successfully grown and fabricated a variety of LDs ranging from violet to green on nonpolar/semipolar orientations.

Figure 4: Far field image of the semipolar (20$\underline{2}$1) laser diode demonstrated at UCSB.

ACKNOWLEDGEMENTS

This work was supported by the Solid State Lighting and Energy Center (SSLEC) at UCSB. A portion of this work was done in the UCSB nanofabrication facility, part of the NSF NNIN network (ECS-0335765), as well as the UCSB MRL, which is supported by the NSF MRSEC program (DMR05-20415). The authors would also like to thank all industrial, postdoctoral, and graduate student researchers involved in this work at the SSLEC.

REFERENCES

[1] S. Chichibu, T. Azuhata, T. Sota, S. Nakamura, *Appl. Phys. Lett.* **69**, 4188 (1996).

[2] F. Bernardini and V. Fiorentino, *Phys. Rev. B* **56**, R10024 (1997).

[3] P. Waltereit, O. Brandt, A. Trampert, H.T. Grahn, J. Menniger, M. Ramsteiner, M. Reiche, K.H. Ploog, *Nature* **406**, 865 (2000).

[4] S.H. Park, *Jpn. J. Appl. Phys.* **42**, L170 (2003).

[5] J. Northrop, *Appl. Phys. Lett.* **95**, 133107 (2009).

[6] M. Funato, A. Kaneta, Y. Kawakami, Y. Enya, M. Ueno, T. Nakamura, *Appl. Phys. Exp.* **3**, 021002 (2010).

[7] M. Adachi, Y. Yoshizumi, Y. Enya, T. Kyono, T. Sumitomo, S. Tokuyama, S. Takagi, K. Sumiyoshi, N. Saga, T. Ikegami, M. Ueno, K. Katayama, T. Nakamura, *Appl. Phys. Exp.* **3**, 121001 (2010).

[8] J. Raring, E. Hall, M. Schmidt, C. Poblenz, B. Li, N. Pfister, D. Feezell, R. Craig, J. Speck, S. DenBaars, S. Nakamura, *SPIE Defense and Security Symposium*, 7686-18 (2010).

[9] S. Yamamoto, Y. Zhao, C.C. Pan, R.B. Chung, K. Fujito, J. Sonoda, S.P. DenBaars, S. Nakamura, *Appl. Phys. Exp.* **3**, 122102 (2010).

[10] http://apps1.eere.energy.gov/buildings/publications/pdfs/ssl/ssl_energy-savings-report_10-30.pdf

[11] M. Krames, O. Shchekin, R. Mueller-Mach, G. Mueller, L. Zhou, G. Harbers, M. Craford, *J. of Disp. Tech.* **3**, 160 (2007).

[12] Y. C. Shen, G. O. Mueller, S. Watanabe, N. F. Gardner, A. Munkholm, M. R. Krames, *Appl. Phys. Lett.* **91**, 141101 (2007).

[13] K. T. Delaney, P. Rinke, and C.G. Van de Walle, *Appl. Phys. Lett.* **94**, 191109 (2009).

[14] J. Hader, J. V. Moloney, S. W. Koch, *Appl. Phys. Lett.* **96**, 221106 (2010).

[15] Q. Dai, Q. Shan, J. Wang, S. Chhajed, J. Cho, E. F. Schubert, M. H. Crawford, D. D. Koleske, M.H. Kim, Y. Park, *Appl. Phys. Lett.* **97**, 133507 (2010).

[16] J. Piprek, *Phys. Stat. Sol. A* **207,** 2217 (2010).

[17] D. Feezell, M. Schmidt, R. Farrell, K. Kim, M. Saito, K. Fujito, D. Cohen, J. Speck, S. DenBaars, S. Nakamura, *Jpn. J. of Appl. Phys.* **46**, L284 (2007).

[18] J. W. Raring, M. C. Schmidt, C. Poblenz, Y.C. Chang, M. J. Mondry, B. Li, J. Iveland, B. Walters, M. R. Krames, R. Craig, P. Rudy, J. S. Speck, S. P. DenBaars, S. Nakamura, *Appl. Phys. Exp.* **3**, 112101 (2010).

[19] K.M. Kelchner, R.M. Farrell, Y.D. Lin, P.S. Hsu, M. T. Hardy, F. Wu, D.A. Cohen, H. Ohta, J. S. Speck, S. Nakamura, S.P. DenBaars, *Appl. Phys. Exp.* **3**, 092103 (2010).

[20] R. M. Farrell, P. S. Hsu, D. A. Haeger, K. Fujito, S. P. DenBaars, J. S. Speck, S. Nakamura1, *Appl. Phys. Lett.* **96**, 231113 (2010).

[21] Y.D. Lin, S. Yamamoto, C.Y. Huang, C.L. Hsiung, F. Wu, K. Fujito, H. Ohta, J.S. Speck, S.P. DenBaars, S. Nakamura, *Appl. Phys. Exp.* **3**, 082001 (2010).

ACRONYMS

LED: Light-Emitting Diode
LD: Laser Diode
SSL: Solid-State Lighting
SSLEC: Solid-State Lighting and Energy Center
UCSB: University of California Santa Barbara
IQE: Internal Quantum Efficiency